Influence of geometric, geologic, geomorphic and subsurface ground conditions on the accuracy of empirical models for prediction of lateral spreading

PBD III VANCOUVER
Earthquake Geotechnical Engineering

J. Russell, S. van Ballegooy & M. Ogden
Tonkin + Taylor, Ltd., Auckland, New Zealand
S. Bastin & M. Cubrinovski
Department of Civil and Natural Resources Engineering – University of Canterbury, Christchurch, New Zealand

ABSTRACT
Liquefaction-induced lateral spreading can result in significant damage to the built environment, as observed in Christchurch during the 2010 to 2011 Canterbury Earthquake Sequence (CES). Predicted Lateral Displacements (LD) from published empirical models have been shown to vary from those measured in parts of Christchurch during the CES by a factor of <0.5 to >2. A widely used empirical method for predicting LD is that proposed by Zhang et al. (2004). Based on a few selected transects along the Avon River in Christchurch, the Zhang et al. (2004) model has been shown by some researchers to provide better agreement between the measured and predicted magnitude and extent of lateral spreading compared to other LD prediction models. Conversely, based on a different set of selected transects along the Avon River, other researchers have shown that the Zhang et al. (2004) empirical model does not provide a good fit between the measured and predicted LD compared to other LD prediction models. The reasons for these apparent contradictory conclusions may result from the varied transect locations and associated geometric, geologic, geomorphic variability and subsurface ground conditions. The objective of this study is to evaluate the combinations of these factors for which the Zhang et al. (2004) empirical model predicts the LD reasonably well and also the conditions for which it does not predict the LD very well. Combining the available datasets outlining horizontal ground surface displacements during the CES, the maximum extent of lateral spreading and the magnitude of maximum displacement has been estimated along the Avon River. By using the extensive Cone Penetration Test (CPT) dataset available, a regional lateral spreading assessment has been undertaken, based on the Zhang et al. (2004) empirical model, to assess the predicted LD along a reach of the Avon River eastward of the Central Business District (CBD). The results have been compared to the measured LD that occurred for the 22 February 2011 earthquake. The results show that the Zhang et al. (2004) model tends to over predict LD more in the older river terrace deposits when compared to the younger reworked river floodplain deposits.

1 INTRODUCTION

Liquefaction and associated lateral spreading caused severe damage to the built environment in Christchurch, New Zealand during the 2010-2011 Canterbury Earthquake Sequence (CES) (Rogers et al., 2015). Severe land damage resulting from lateral spreading occurred during the 4 September 2010 (M_w 7.1), 22 February 2011 (M_w 6.2), 13 June 2011 (M_w 5.6 followed by a M_w 6.0 event) and 23 December 2011 (M_w 5.8 followed by a M_w 5.9 event) events. Figure 1 shows the observations of liquefaction and lateral spreading during the CES. Lateral spreading typically occurred in the eastern areas of Christchurch adjacent to the Avon River. In the case study area shown in Figure 1 the largest modelled Peak Ground Accelerations (PGA) occurred during the February 2011 earthquake. These ranged from approximately 0.3 to 0.6 g (Bradley and Hughes, 2012).

There are a number of empirical methods available to predict the magnitude of ground displacements resulting from lateral spreading (including Youd et al., 2002 and Zhang et al., 2004) that could occur during earthquake shaking. The primary benefit of the empirical methods are that they are relatively simple and less time intensive to implement compared to more advanced computational methods such as Newmark type sliding block analyses.

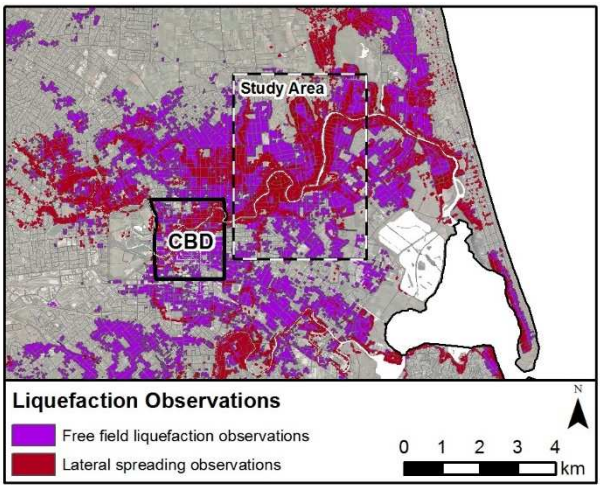

Figure 1. Map indicating the areas affected by liquefaction and lateral spreading observed during the CES.

The displacement estimates produced from the empirical models have been shown to vary by as much as a factor of 0.5 to 2 from those measured in parts of Christchurch following the CES (Bowen et al., 2012, Deterling, 2015, Cubrinovski & Robinson 2015). Bowen et al. (2012) concluded that the Youd et al. (2002) method generally over-predicted lateral spread displacement

magnitude at large distances from the free face. Whereas, Deterling et al. (2015) undertook transects on the lower reaches of the Avon River in the suburbs of Avondale, Burwood, Aranui and New Brighton and found that the Youd et al. (2002) methodology tended to under predict lateral spreading displacements and that the Zhang et al. (2002) methodology generally performed better than other methods. Robinson et al. (2013) undertook transects in the Avon Loop and found that the Youd et al. (2002) methodology tends to over predict LD by more than a factor of two. The different studies examined different cross-sections in different geological and geomorphological areas, which may account for some of the variability in the conclusions reached. Bastin et al. (2017), a companion paper to this paper, demonstrates that geology and geomorphology play an important role in the extent and magnitude of lateral spreading.

This study applies the Zhang et al. (2004) empirical model to a case study area of Christchurch (shown in Figure 1). The Zhang et al. (2004) methodology was adopted because it was developed relatively recently and is simple to apply to a CPT based dataset, such as that available for Christchurch. In contrast to previous studies, that focused on selected transects only, this study considers a wider case study area with varying geology, geomorphology and severity of lateral spreading (i.e. ranging from no lateral spreading to severe lateral spreading).

The Zhang et al. (2004) model is applied to the available Cone Penetration Test (CPT) data within the study area to predict the magnitude of Lateral Displacement (LD) at each CPT location for the February 2011 earthquake. The predicted LD estimates are then compared with measured displacements, determined either through LiDAR or satellite imagery. LD estimates at each CPT location are then grouped into geomorphic zones to examine the influences of geomorphology and near-surface sediment variability on the accuracy and precision of the Zhang et al. (2004) methodology. The February 2011 earthquake was selected for analysis as it was the earthquake event in the CES for which extensive lateral spreading occurred within the case study area and because it also had the most extensive set of measured LD values.

2 BACKGROUND

2.1 Geological Setting within the context of Liquefaction Hazard

A description of the local geology and geological history of Christchurch is available in Brown and Webber (1992). In summary, Christchurch is situated on an alluvial flood plain on the east coast of New Zealand's South Island. The western suburbs are typically underlain by near surface gravels that are generally not susceptible to liquefaction. Alluvial silts and sands with areas of drained peat swamps predominantly underlie the central and eastern suburbs. Dune and estuarine sands and silts are present adjacent to the eastern coastline. The loose sands and silts in eastern Christchurch are generally susceptible to liquefaction. Several meandering rivers and streams are present within Christchurch, including the Avon and Heathcote rivers. Groundwater in the areas adjacent to these rivers is shallow, typically within 3m of the ground surface (van Ballegooy et al., 2014). The ground conditions and low-lying elevations east of the Christchurch Central Business District (CBD) result in land that is vulnerable to lateral spreading under ground shaking, as observed during the CES (Figure 1).

2.2 Available Data

The data used for this study includes:

- The geomorphological map developed by Bastin et al. (2017);
- CPT data from the New Zealand Geotechnical Database (NZGD, 2017) downloaded on 29 April 2016;
- The February 2011 earthquake PGA contour model developed by Bradley and Hughes (2012);
- The February 2011 earthquake event specific groundwater model developed by van Ballegooy et al. (2014);
- The post February 2011 earthquake LiDAR derived horizontal displacements as described in T+T (2015); and
- The post February 2011 satellite imagery derived horizontal displacements from Martin and Rathje (2014).

Note that, CPT affected by predrill below the ground water table and CPT having a depth less than 5m have been excluded from the CPT dataset.

2.3 Zhang et al. (2004) Model

The Zhang et al. (2004) method is based on estimating the induced cyclic shear stress for a given level of earthquake shaking from CPT data and then empirically correlating with geometric effects. The Zhang (2004) model for free-face conditions is as shown in Equation 1.

$$LD = 6\left(\frac{L}{H}\right)^{-0.8} LDI \quad [1]$$

Where LD = Lateral Displacement (mm); L = the distance from the base of the free-face to the point of interest; H = free-face height; and LDI = Lateral Displacement Index (mm) and is calculated as shown in Equation 2.

$$LDI = \int_0^{Z_{max}} \gamma_{max} dz \quad [2]$$

Where Z_{max} is typically taken as 2H and γ_{max} is the maximum cyclic shear strain derived from liquefaction triggering assessment coupled with the Zhang et al. (2004) maximum cyclic shear strain empirical equations.

Because it is based on a single CPT point location, the Zhang et al. (2004) model is a simple one dimensional assessment method. This means that it does not account for the spatial variability of the surrounding land.

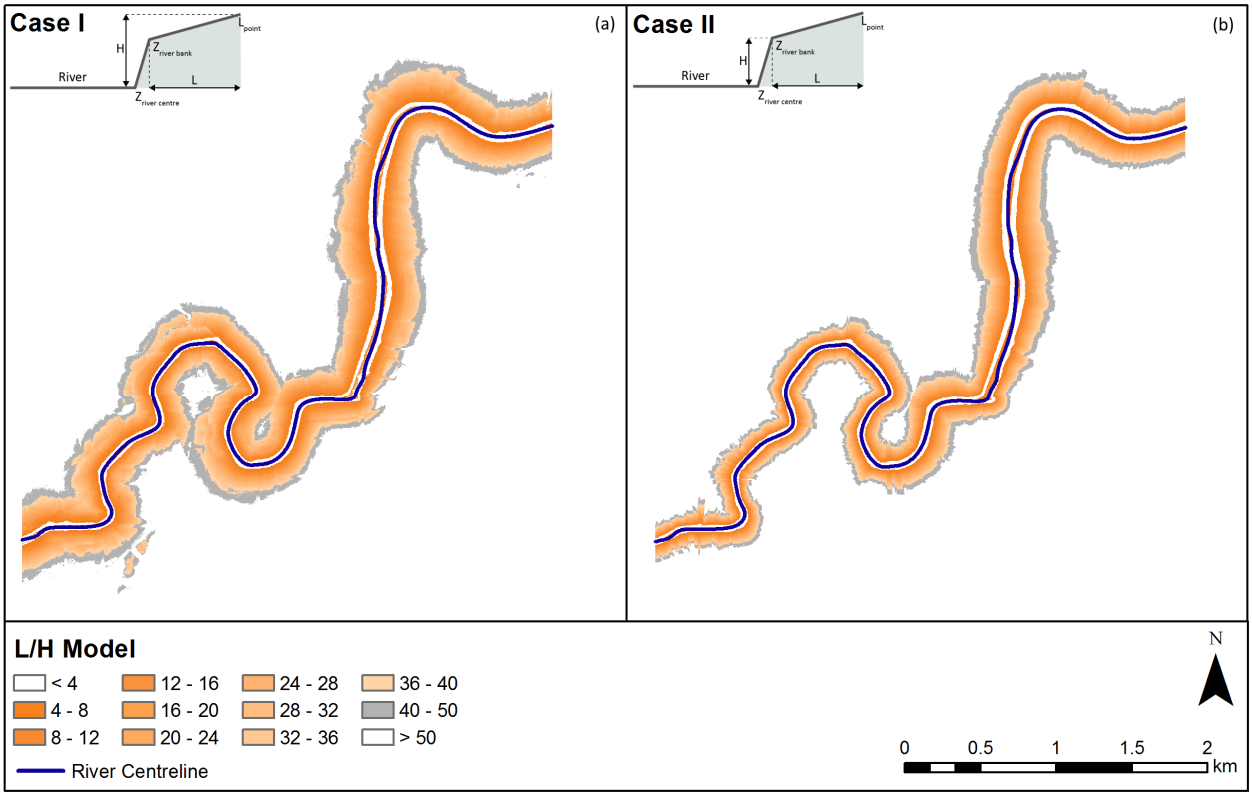

Figure 2: L/H models within the study area along the Avon River. (a) Case I and (b) Case II.

3 METHODOLOGY

3.1 Case Study Area

The case study area, shown in Figure 1, is to the north east of the Christchurch CBD and includes portions of the suburbs of Avonside, Avondale, Dallington and Burwood. It includes a reach of the Avon River that was affected by moderate-to-severe lateral spreading during the CES. The case study area closely aligns with the spatial coverage of satellite imagery derived horizontal displacements. The study area has good variability in geology, geomorphology, topography and land performance during the CES.

3.2 Estimating Length to Height (L/H) Ratio

L/H was estimated at each CPT location by building a three dimensional (3D) model of the river channel which was developed from river cross-sectional data obtained by surveys commissioned by Christchurch City Council (CCC) in 2008. The 3D model of the river was embedded into a Digital Elevation Model (DEM) of the ground surface developed from a 2003 LiDAR survey to provide a combined bathymetric and topographic model. The river channel invert was manually identified from the combined bathymetric and topographic model by identifying the lowest point in the 3D model of the river channel. The top of the riverbank was manually identified from the DEM and aerial imagery.

The study area was then divided into a grid comprising 2.5 m by 2.5 m cells, and L/H was calculated for each cell. As shown in Figure 2, two methods of calculating L/H have been used in this study, referred to as Case I and Case II respectively. Both Case I and Case II have the same L, which for the purpose of this study is the shortest distance between the center of each cell and the top of the river bank determined through Euclidean geometry. This method tends to result in an under estimation of L because, as defined in Zhang et al. (2004), L should be measured from the bottom of the riverbank. However, this method was adopted due to the relative difficulty and uncertainty associated with identifying the base of the riverbank. It is acknowledged that this tends to result in an over-prediction of LD, with the effect of over-prediction being more significant closer to the river (where there are smaller L/H values) but less significant further away from the river (where there are larger L/H values).

Case I estimates H as the relative elevation difference between the grid cell and the elevation of the nearest point on the river invert line whereas Case II estimates H as the relative elevation difference between the nearest point on the top of the riverbank and the nearest point on the river invert line. While the method of estimating H in Case II aligns more closely with the method proposed by Zhang et al. (2004), including Case I in the analyses provides some variance in the estimated LD where Case I provides an upper bound and Case II a lower bound estimate.

The LD model in Zhang et al. (2004) gives an L/H range between 4 and 40. This study extends the range to include the data points between 40 and 50, which enables testing of the method beyond the originally intended range.

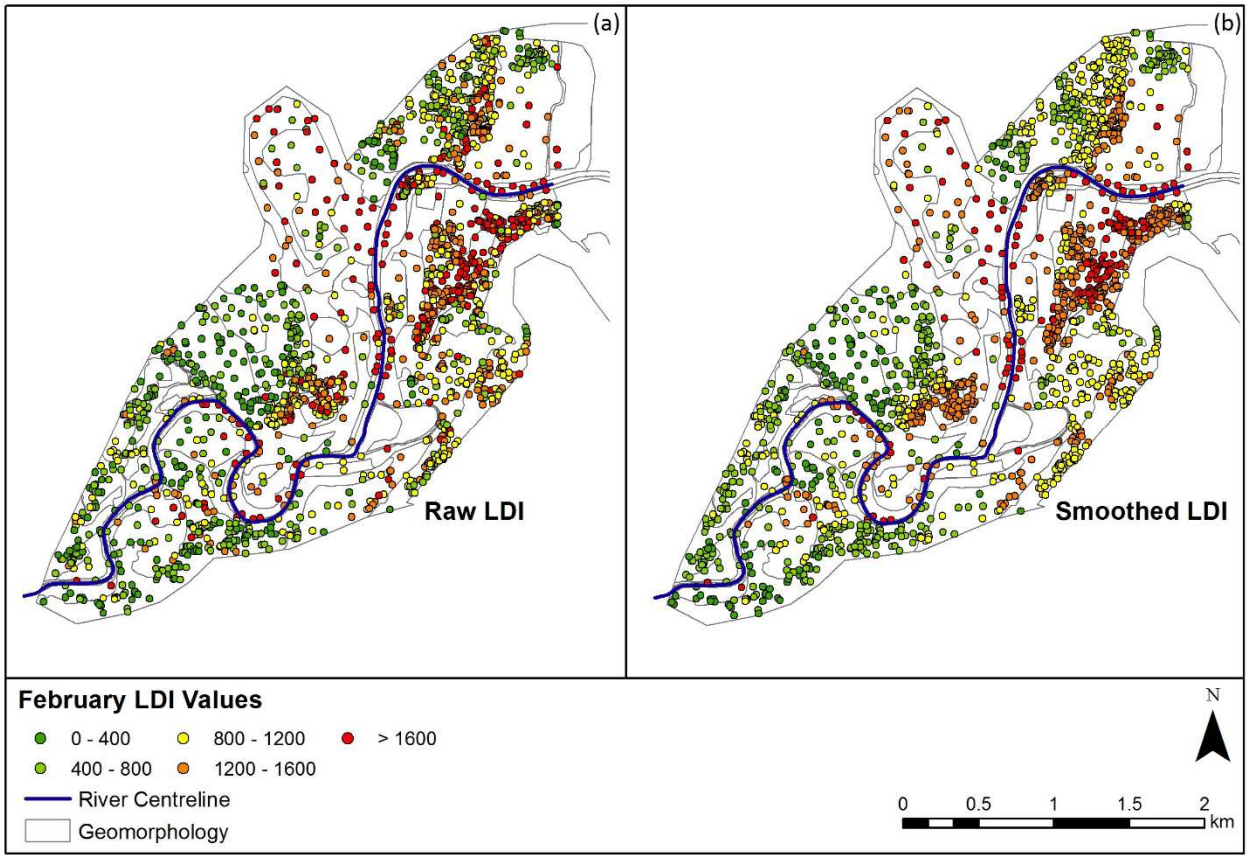

Figure 3: Calculated LDI values overlaid on the different geomorphic zones. (a) presents raw values and (b) presents spatially smoothed values.

The L/H model is a simplified geometric characterization of the topography for a single free face. However, it is noted that throughout the study area there are terrace risers providing a secondary free face that are not adequately taken into account in the L/H models. Further refinements to the L/H model can be made by mapping additional topographical features which provide a free face or slope for which lateral spreading can occur. For the purposes of this study, these additional topographic features have been ignored. The effect of this limitation is discussed further in Section 5.

3.3 Geomorphic Characterization

As noted in Section 1, in conjunction with this study, a complimentary study that included the geomorphic characterization of the land within the study area has been undertaken (see Bastin et al., 2017 for detailed descriptions of the geomorphic units). The geomorphologic zones present within the study area include flood plains both proximal and distal to the Avon River, terraces comprising older deposits, along with paleo-channels and swamps. The polygons of the different geomorphic zones can be seen in Figure 3. This geomorphic characterization was used to group CPTs within the study area to examine whether the accuracy and precision of the Zhang et al. (2004) methodology is influenced by geomorphology.

3.4 Calculating Lateral Displacement Index (LDI)

For this study, LDI has been calculated using the CPT dataset outlined in Section 2.2. Estimates of both the factor of safety against liquefaction triggering (FS_{LIQ}) and the relative density (D_r) are needed to calculate γ_{max} as shown in Equation 2. For the purposes of this study FS_{LIQ} has been calculated using the Boulanger and Idriss (2014) methodology. The soil behaviour-type index (I_c) threshold of greater than 2.6 was applied, above which the soil was assumed too plastic in behaviour to liquefy (Robertson and Wride, 1998). The Fines Content (FC) was estimated from the I_c using the default Boulanger and Idriss (2014) correlation with a fitting parameter C_{FC} value of 0. Further analysis will incorporate the FC correlation derived for the Avon River by Cubrinovski and Robinson (2016). D_r was calculated from q_c based on the approach described in Zhang et al. (2004).

To simplify the calculation of LDI, Z_{max} is set to 10 m. Because H in this area is typically between 4 to 5 m and it is typical practice to limit Z_{max} to 2H this assumption will generally result in slightly higher values of LDI. The effects of this assumption are discussed further in Section 5.

Figure 3 presents the results of the LDI calculation. The "Raw" LDI shown on Figure 3(a) have been calculated using the standard methodology derived by Zhang et al (2004) To calculate the "Smoothed" LDI shown on Figure 3(b), the CPTs are classified into geomorphic units that are

described in Section 3.3, then the LDIs for all CPTs within a 100 m radius of a given CPT are averaged.

The smoothing process has been adopted in an attempt to address the spatial variability of ground conditions. Where ground conditions are spatially variable, spatially varying LDIs are calculated which in turn results in spatially variable LD estimates. However, lateral spreading occurs as a system rather than in thin transect slices. That is if soil conditions parallel with the river (upstream and downstream) are better, then the point in question will tend to sustain less actual LD than predicted. Conversely, if adjacent soil conditions are worse, the actual LD will be greater than predicted.

While spatial smoothing improves the LD predictions when considering spatial variability in the direction parallel with the river, the smoothing process does not appropriately handle spatial variability perpendicular to the river. That is, if soil conditions immediately adjacent to the river free face are such that liquefaction is unlikely to occur, and hence the LDI is very low, then lateral spreading is also unlikely to occur, even if further back from the river the calculated LDI values are very high. This is because the non-liquefying soil immediately adjacent to the free face prevents LD from occurring. Bastin et al (2017) demonstrates some examples of this within the case study area by identifying some key transects along the Avon River. The effect of this limitation is discussed further in Section 5.

3.5 Calculating predicted Lateral Displacement (LD)

By extracting the results from the L/H models shown in Figure 2 and LDI values shown in Figure 3 and applying Equation 1 four different combinations of predicted LD were calculated as follows:

- L/H Case I and Raw LDI;
- L/H Case I and Smoothed LDI;
- L/H Case II and Raw LDI; and
- L/H Case II and Smoothed LDI.

The results of the calculated LD for each combination are shown in Figure 4 and discussed in Section 4.

3.6 Estimating Actual Movement

For the purposes of this study two methods were used to provide an estimate of the actual horizontal movement induced by lateral spreading as a result of the February 2011 earthquake, namely a LiDAR survey based method and a satellite imagery based method. The LiDAR survey based estimate is derived using a sub-pixel correlation method developed by Imagin' Land Corporation and the California Institute of Technology (Beavan et al., 2012a). The satellite imagery based estimate of lateral movement is derived using an optical imagery correlation process described in Martin and Rathje (2014). For both methods, the process applied gives a "measured" lateral displacement on a 16 m x 16 m grid. Due to the relatively limited availability of suitable overlapping satellite imagery before and after the February 2011 earthquake, a smaller area than the LiDAR imagery was analyzed using this method.

Where available, estimates of the total liquefaction induced horizontal movement for both of these methods were extracted for each CPT location and compared to the LD values that were calculated for the February 2011 earthquake (Figure 4). It is important to note that the measured horizontal displacements were not always perpendicular to the river (as shown in Bastin et al. 2017). The LD estimates from the Zhang et al. (2004) method are derived on the assumption that the direction of the LD is perpendicular to the free face. This assumption can lead to potentially higher measured values compared to the predicted values.

4 RESULTS

Figure 4 shows the results of the analyses. The estimated LD values based on the Case I and Case II L/H models are presented on the same axis and differentiated by different colors. Figure 4(a) plots LD calculated from raw LDI vs. LiDAR derived horizontal displacements, Figure 4(b) plots LD calculated from smooth LDI vs. LiDAR derived horizontal displacements, Figure 4(c) plots LD calculated from raw LDI vs. satellite derived horizontal displacements and Figure 4(d) plots LD calculated from smooth LDI vs. satellite derived horizontal displacements. For reference, lines showing 0.5:1 (under-prediction), 1:1 (correct prediction) and 2:1 (over-prediction) are shown with the number and percentage of CPT points falling within each sector shown.

In general, the data exhibits a high degree of scatter either side of the 1:1 line indicating a relatively poor correlation between the predicted and measured LD values. Closer inspection of Figure 4 shows that a greater proportion of predicted LD tend to be higher than the observed LD values.

4.1 LiDAR Survey Derived Horizontal Displacements

Figure 4(a) shows that for the raw LDI, 50% and 52% of the points for Case I and Case II respectively are contained within the 0.5:1 and 2:1 lines. Furthermore, 70% of the points for both Case I and Case II plot above the 1:1 line. Figure 4(b) shows that the smoothed LDI exhibits similar trends with 57% and 59% of the points for Case I and II respectively contained with the 0.5:1 and 2:1 lines. Furthermore, 77% of points for both Case I and Case II plot above the 1:1 line.

4.2 Satellite Imagery Derived Horizontal Displacements

Figure 4(c) shows that for the raw LDI, 34% and 38% of points for Case I and Case II respectively are contained within the 0.5:1 and 2:1 lines. Furthermore, 72% and 73% of the points for Case I and Case II respectively plot above the 1:1 line. Figure 4(d) shows, as with the LiDAR derived horizontal movements, the smoothed LDI exhibits similar trends with 36% and 41% of the points for Case I and II respectively contained with the 0.5:1 and 2:1 lines. Furthermore, 78% and 81% of points for Case I and Case II respectively plot above the 1:1 line

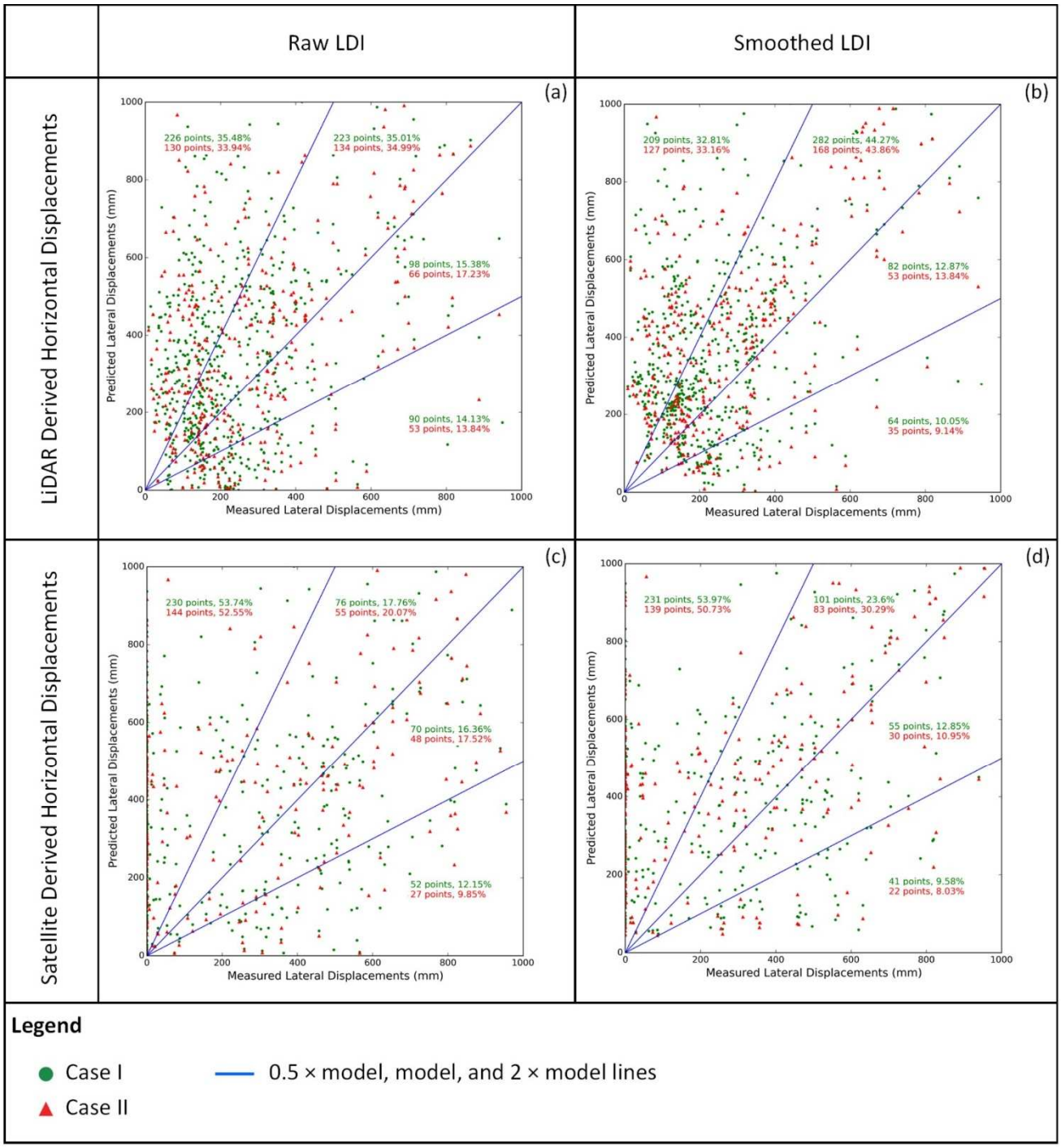

Figure 4: Comparison of the predicted and measured LD values for LiDAR survey and Satellite imagery derived horizontal displacements.

5 DISCUSSION

5.1 Reasons for Variability between Predicted and Measured LD values

Figure 4 shows considerable variability between the predicted and measured LD values. There are uncertainties and several inherent limitations of the methodology that has been used to estimate LD from the CPT dataset that will influence the results. First, the L/H model has been built based on the bathymetric and topographic information collected prior to the September 2010 earthquake. Because there was ground surface subsidence in some parts of the study area during the September 2010 earthquake, adopting the pre-September 2010 model will tend to over-predict H in areas where

liquefaction and lateral spreading occurred in the September 2010 earthquake. This affects approximately 50% of the study area, and in turn, results in an over-prediction of LD using the Zhang et al. (2004) model.

Second, to simplify the calculation Z_{max} was assumed to be 10 m rather than the typical practice of adopting 2H. Given that the free face height in this reach of the river tends to be between 4 to 5 m, adopting Z_{max} = 10 m will tend to result in higher values of LDI than if 2H were adopted. This in turn will also result in an over-prediction of LD using the Zhang et al. (2004) model.

Third, because the methodology used to calculate the Case I L/H model results in higher values of H at the same value of L it tends to produce higher values of predicted LD. This is reflected in Figure 4 as a tendency for over-prediction relative to the measured LD. Furthermore, L is taken to the top of the riverbank rather than the base of the river bank as per the Zhang et al. (2004) method. This results in an under prediction of L and over prediction of LD.

Fourth, excluding the minor topographic features from the L/H model that could have caused LD will tend to result in an under prediction of LD using the Zhang et al. (2004) model.

Fifth, as discussed in Section 3.6 the LD estimates from the Zhang et al. (2004) method are derived with the assumption that the direction of the LD is perpendicular to the free face. However, actual LD did not always occur perpendicular to the free face. Where this occurred, the measured LD will be larger than the actual component against which the predicted LD should be compared.

Sixth, uncertainty inherent in the groundwater model PGA model and inherent measurement error in the LiDAR and satellite derived horizontal displacements introduces further scatter into the data.

The majority of these factors result in higher values of LD being predicted and this may explain why the majority of the points are plotted above the 1:1 line in Figure 4. Furthermore, all of the factors contribute to the scatter observed in Figure 4.

5.2 Raw vs. Smoothed LDI

When compared with the raw methodology, adopting a smoothed approach to the calculation of LDI (as described in Section 3.4) has tended to result in an improvement in the number of points plotting between the 0.5:1 and 2:1 lines. While this improvement is minor it does indicate that improvement can be made in the Zhang et al. (2004) methodology by considering the performance of the land as a system rather than as an individual point. Further investigation into the smoothing process by considering other functions for spatially averaging the LDI for a geomorphic grouping may result in further improvement.

However, there is still considerable scatter in the plots for the smoothed approach. This suggests that there are other important factors not captured by this smoothing approach. Bastin et al. (2017) provide some insight into this problem as it concludes that the thickness and continuity of liquefying layers has a strong influence on the tendency for lateral spread to occur. Thick, continuous liquefying layers tend to result in larger LD values, while thin, discontinuous liquefying layers tend to result in smaller LD values. The smoothing approach adopted has a limited capacity to capture both continuity and thickness of liquefiable layers.

5.3 Geomorphic characterization

The geomorphic characertization undertaken by Bastin et al. (2017) can be used to investigate the accuracy and precision of the Zhang et al. (2004) methodology within different geomorphological areas. The two geomorphic classifications containing the largest number of CPT in the study area are the terraces and floodplains. Figure 5 shows a comparison of predicted versus measured LD values for CPT within these two geomorphic zones, using smoothed LDIs calculated from Case II L/H and LiDAR derived horizontal displacements.

Inspection of Figure 5 reveals that, terraced

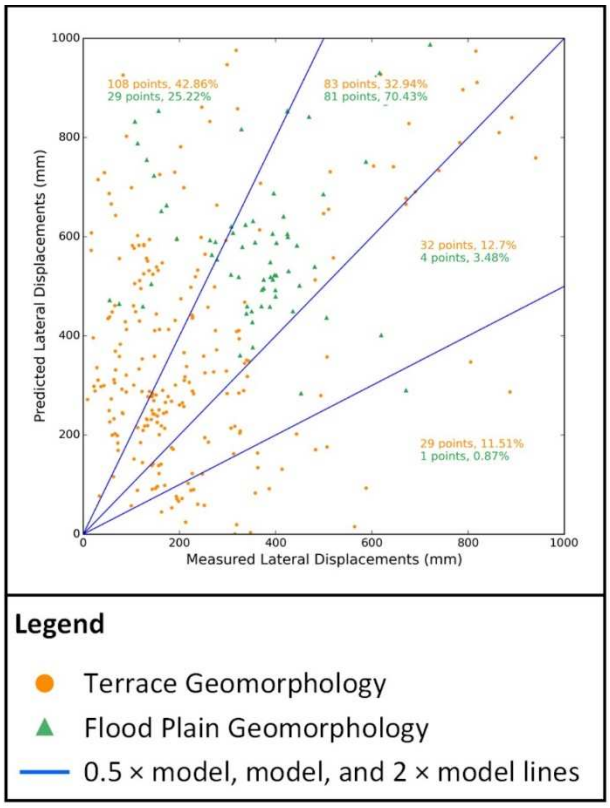

Figure 5: Comparison of the predicted and measured LD values for LiDAR derived horizontal displacements using a smoothed LDI dataset separated by geomorphology.

geomorphology has 46% of points are contained within the 0.5:1 to 2:1 lines and 76% of points are plotted above the 1:1 line. Whereas for flood plain geomorphology, 74% are contained within the 0.5:1 to 2:1 lines and 96% of points are plotted above the 1:1 line. Figure 5 shows a considerable improvement in the Zhang et al. (2004) methodology for predicting LD for the CPT within the active flood plain of the river. This is demonstrated by the relatively tight grouping of CPT points within the 1:1 and 2:1 lines – accounting for 70% of CPT points. In contrast, for the CPT located on terraced geomorphology 46% plot

within the 0.5:1 to 2:1 lines. This observation is also supported by Bastin et al. (2017) which concludes that lateral spreading is strongly influenced by local variability such that lateral spreading tends to be confined to the younger soils on the low to mid elevation flood-plains with negligible to no observations of lateral spreading in the remnant higher elevation terraces proximal to the river bank.

6 CONCLUSIONS

This study has demonstrated that, when applied to the case study area under consideration, predictions of LD using the Zhang et al. (2004) methodology show considerable scatter when compared to measured LD values using both LiDAR survey and Satellite imagery data from the CES. In general, the implementation of the methodology tends to over-predict LD relative to the measured LD. The results were largely insensitive to the definition of H, and hence L/H.

Furthermore, consideration of the performance of the land as a system by smoothing the LDI values within the geomorphological groups has demonstrated a minor improvement in the prediction of LD using the Zhang et al. (2004) methodology. Further optimization of this approach may result in further improvement in the accuracy of the Zhang et al. (2004) methodology. An important factor for further consideration is whether there is horizontal continuity of liquefying soil layers.

Finally, consideration of the CPT points by geomorphic groups has indicated that the Zhang et al. (2004) methodology tends to provide an improved correlation of predicted vs. measured LD for the younger soils of the alluvial flood plain compared with the older river terrace deposits. This should be considered by practicing engineers applying the Zhang et al. (2004) methodology and is a potential avenue for further improvement of the method.

Additional work is planned to conduct detailed characterization of the geomorphic areas and areas that did and did not laterally spread and further examine the mechanism facilitating lateral spreading.

7 ACKNOWLEDGEMENTS

This project was supported by QuakeCoRE, a New Zealand Tertiary Education Commission-funded Centre. This is QuakeCoRE publication number 0142. The Ministry of Building, Innovation and Employment provided additional support for supplementary CPT within the study area.

8 REFERENCES

Beaven, J., Levick, S., Lee, J. and Jones, K., 2012a. *Ground displacements and dilatational strains caused by the 2010 – 2011 Canterbury Earthquakes.* GNS Science (Consultancy report 2012.67), GNS Science, Lower Hutt.

Beavan, J., Motagh, M., Fielding, E., Donelly, N. and Collett, D. 2012b. Fault slip models of the 2010 – 2011 Canerbury, New Zealand, earthquakes from geodetic data and observations of post-seismic ground deformation. New Zealand Journal of Geology and Geophysics, 55(3):207-221.

Bastin, S., Cubrinovski, M., van Ballegooy, S. and Russell, J., 2017. Geologic and Geomorphic Influences on the Spatial Extent of Lateral Spreading in Christchurch New Zealand, 3rd International Conference on Performance-based Design in Earthquake Geotechnical Engineering, ISSMGE-TC203, Vancouver, BC, Canada.

Bowen, H., Jacka, M., van Ballegooy, S., and Sinclair, T. 2012. Lateral spreading in the Canterbury earthquake - observations and empirical prediction methods. Proceedings, 15th World Conference on Earthquake Engineering, IAEE, Lisboa, Portugal.

Boulanger, R. and Idriss, I. 2014. CPT and SPT based liquefaction triggering procedures, Report No. UCD/CGM-14/01. Center for Geotechnical Modeling, Department of Civil and Environmental Engineering, University of California Davis, California.

Bradley, B.A. and Hughes, M., 2012. "Conditional Peak Ground Accelerations in the Canterbury Earthquakes for Conventional Liquefaction Assessment", Technical Report Prepared for the Department of Building and Housing, 22 pp.

Brown, L. and Weeber, J. 1992. Geology of the Christchurch Urban Area. Scale 1:25 000. Institute of Geological and Nuclear Sciences geological map 1. 1 sheet + 105 p, Lower Hutt, New Zealand.

Deterling, O., 2015. Factors influencing the lateral spread displacements from the 2011 Christchurch, New Zealand earthquake. M.Sc. in Engineering Thesis, University of Texas at Austin, United States of America

Martin, J. G. & Rathje, E. M., 2014. Lateral Spread Deformations from the 2011 Christchurch, New Zealand Earthquake Measured from Satellite Images and Optical Image Correlation. 10th National Conference in Earthquake Engineering, Earthquake Engineering Research Institute (EERI), Anchorage, AK, USA.

NZGD, 2017. New Zealand Geotechnical Database. Accessed from www.nzgd.org.nz.

Robinson, K., Cubrinovski, M. & Bradley, B.A., 2013. Sensitivity of predicted liquefaction-induced lateral displacement from the 2010 Darfield and 2011 Christchurch Earthquakes. *New Zealand Society for Earthquake Engineering Technical Conference and AGM, 2013,* Wellington, New Zealand.

Rogers, N., van Ballegooy, S., Williams, K., & Johnson, L. 2015. Considering Post-Disaster Damage to Residential Buidling Construction - Is Our Modern Building Construction Resilient? *6th International Conference on Earthquake Geotechnical Engineering 2015*, ISSMGE, Christchurch, New Zealand.

Tonkin and Taylor, 2013. *Liquefaction Vulnerability Study. Report prepared for the Earthquake Commission, New Zealand.*

Tonkin + Taylor, 2015. *Canterbury Earthquake Sequence: Increased Liquefaction Vulnerability Assessment Methodology*. Report prepared for the Earthquake Commission, New Zealand.

Van Ballegooy, S., Cox, S.C., Thurlow, C., Rutter, H.K., Reynolds, T., Harrington, G., Fraser, J. & Smith, T., 2014. *Median water table elevation in Christchurch and surrounding areas after the 4th September 2010 Darfield Earthquake - Version 2.* (GNS Science report 2014/18). Institute of Geological and Nuclear Sciences, Lower Hutt, New Zealand.

Youd, T.L., Hansen, C.M., and Bartlett, S.F., 2002. Revised multilinear regression equations for prediction of lateral spread displacement, *Journal of Geotechnical and Geoenvironmental Engineering*, 128(12), 1007-1017.

Zhang, G., Robertson, P. K. & Brachman, R. W. I., 2004. Estimating Liquefaction-Induced LDs Using the Standard Penetration Test of Cone Penetration Test. *Journal of Geotechnical and Geoenvironmental Engineering*, 8(130): 861-871.